

Mapping of rainfall-induced landslide susceptibility in Wencheng, China, using support vector machine

Cheng Su · Lili Wang · Xizhi Wang · Zhicai Huang · Xiaocan Zhang

Received: 14 May 2014 / Accepted: 18 December 2014 / Published online: 10 January 2015
© Springer Science+Business Media Dordrecht 2015

Abstract This study presents a framework for mapping rainfall-induced landslide susceptibility in the Wencheng area of Zhejiang Province, China, using support vector machine (SVM). Seven conditioning factors of elevation, slope, aspect, distance to roads, lithology, land use, and normalized difference vegetation index selected by correlation analyses, and two triggering factors of daily and cumulative rainfall data were employed as input data in the SVM modeling. The training dataset was constructed using 354 landslide inventories identified from field surveys between 1981 and 2010, and 354 points not prone to slides selected as positive and negative samples, respectively, based on a statistical method of factors. A fivefold cross-validation and receiver operation characteristic were applied to evaluate the performances of the SVM model. The summarized area under the curve result was 0.96, indicating that SVM demonstrated good and stable performance in mapping landslide susceptibility. Two practical cases were investigated: the Trami typhoon of August 22, 2013, and the Kong-Re typhoon of August 26, 2013, which brought heavy rainfall of 300 and 111 mm, respectively, to the Wencheng area. The resulting maps showed that SVM could provide a map with high probability values over small areas, demonstrating good properties of generalization. In addition, mapping of landslide susceptibility could be converted easily into landslide warning by replacing the triggering factor with weather forecasting data. Landslide susceptibility maps based on the results of

C. Su · L. Wang · X. Wang · Z. Huang · X. Zhang (✉)
Institute of Space Information and Technique, Department of Earth Sciences, College of Science,
Zhejiang University, Hangzhou 310027, China
e-mail: zxc1121@zju.edu.cn

C. Su
e-mail: sc20184@zju.edu.cn

L. Wang
e-mail: ongleilei@163.com

X. Wang
e-mail: yvonnewxz826@163.com

Z. Huang
e-mail: hzc@zju.edu.cn

this study could be used to assist governments and planners, and help reduce the economic and social costs of rainfall-induced landslides.

Keywords Landslide susceptibility · Rainfall · Support vector machine · Receiver operation characteristic · GIS · China

1 Introduction

Landslides are major geological hazards that occur throughout the world, causing thousands of fatalities and damage to property worth billions of US dollars each year. Furthermore, the rate of occurrence of landslides and the scale of associated fatalities and socioeconomic losses have increased over recent years. Therefore, a map of landslide susceptibility is crucial for helping planners both select favorable locations for development schemes and take suitable mitigating action before landslides devastate a region.

Many researchers have developed techniques for constructing maps of landslide susceptibility (Aleotti and Chowdhury 1999; Brenning 2005; Carrara et al. 1991, 1995; Chacón et al. 2006; Corominas and Moya 2008; Guzzetti et al. 1999; Hong et al. 2007; Oh et al. 2009; van Westen et al. 2006, 2008; Varnes 1984; Ward 1945). There have been hundreds of studies on landslide susceptibility mapping, and most have advocated parametric statistical techniques such as bivariate or multivariate statistical analyses (Althuwaynee et al. 2012; Baeza and Corominas 2001; Carrara et al. 2003; Devkota et al. 2013; Nandi and Shakoor 2010; Schicker and Moon 2012; van Westen et al. 1997; Yilmaz et al. 2012), logistic regression (Ayalew and Yamagishi 2005; Bai et al. 2010; Chau et al. 2004; Dai and Lee 2002; Das et al. 2010; Lee 2005; Lee and Min 2001; Ohlmacher and Davis 2003; Pourghasemi et al. 2013; van den Eeckhaut et al. 2006), frequency ratio (Akgun et al. 2008; Lee and Pradhan 2006; Pradhan et al. 2011; Vijith and Madhu 2007), weights of evidence (Dahal et al. 2008; Kayastha et al. 2012; Neuhäuser and Terhorst 2007), or various combinations of the above (Althuwaynee et al. 2014b; Umar et al. 2014). These models have limitations such as strict data distributions, independence of predictors, and nonlinearity, which frequently are not met in practice (Ballabio and Sterlacchini 2012). Therefore, other new methods have been applied for landslide susceptibility mapping using data mining and machine learning approaches, such as fuzzy logic (Akgun et al. 2012; Ercanoglu and Gokceoglu 2002; Kanungo et al. 2006; Pourghasemi et al. 2012; Pradhan 2011; Tangestani 2009), neuro-fuzzy (Pradhan 2013; Pradhan and Lee 2010a; Pradhan et al. 2010a), decision tree methods (Nefeslioglu et al. 2010; Saito et al. 2009; Tien Bui et al. 2012a; Yeon et al. 2010), evidential belief function model (Althuwaynee et al. 2012, 2014a; Tien Bui et al. 2012b), artificial neural network models (Choi et al. 2012; Ermini et al. 2005; Gómez and Kavzoglu 2005; Lee et al. 2006; Nourani et al. 2013; Pourghasemi et al. 2012; Pradhan and Lee 2010a, b; Pradhan et al. 2010b), and support vector machine (SVM) (Ballabio and Sterlacchini 2012; Guo et al. 2005; Marjanović et al. 2011; Tehrani et al. 2014; Tien Bui et al. 2012a; Yao et al. 2008; Yuan et al. 2006). Comparative studies (Falaschi et al. 2009; Lee and Pradhan 2007; Mohammady et al. 2012; Ozdemir and Altural 2013; Pradhan 2013; Pradhan and Lee 2010a, b; Tangestani 2009; Tien Bui et al. 2012a, b; Yesilnacar and Topal 2005; Yilmaz 2009) have shown that these approaches could give rise to qualitative and quantitative improvement in landslide susceptibility mapping relative to traditional statistical techniques. By considering the features of SVM

such as the structure risk minimizing principle, guaranteeing that the best classification hyperplane can be found in mathematical theory, the application of the kernel trick means that SVM can deal with the nonlinearity problem when applied to small samples. Therefore, SVM is a better option for producing objective and stable landslide susceptibility maps, when addressing the high-dimensional nonlinearity problem associated with few training samples.

One of the basic assumptions of the techniques for landslide susceptibility mapping described above is the identification of areas prone to a particular combination of physical properties that could lead to similar events in the future. These physical properties can be divided into two categories: conditioning factors such as slope, lithology, and land use; triggering factors such as rainfall, rapid snowmelt, volcanic eruptions, earthquakes, and anthropogenic activity (Zêzere et al. 1999). Because most landslides are triggered by rainfall, it is necessary to improve the prediction of rainfall-induced landslides (Chang et al. 2008).

Chang and Chiang (2009) provided an informative review and categorized the techniques for rainfall-induced landslides prediction into three classes: (1) correlation analyses, (2) critical rainfall models, and (3) statistical techniques. The first two use historical data or steady-state hydrological concepts and infinite slope stability models to attempt to establish rainfall thresholds likely to trigger landslides. However, they fail frequently because of the lack of data for nonlandslide areas or other important parameters. Statistical techniques could assess landslide susceptibility using many conditioning factors that could be acquired, but few include rainfall as an explanatory variable because of the lack of reliable and accurate rainfall fields.

In this work, a study on the application of the SVM method to the mapping of landslide susceptibility is performed. Rainfall is considered as an explanatory variable in the form of precipitation on the day and for the 4 days prior to the event. Wencheng in southeastern China was selected as the study area because landslides here are typically rainfall induced. To assess the performance of the method, a fivefold cross-validation and receiver operation characteristic (ROC) were applied to two practical cases: the Trami typhoon of August 22, 2013, and the Kong-Re typhoon of August 26, 2013, which brought daily precipitation of

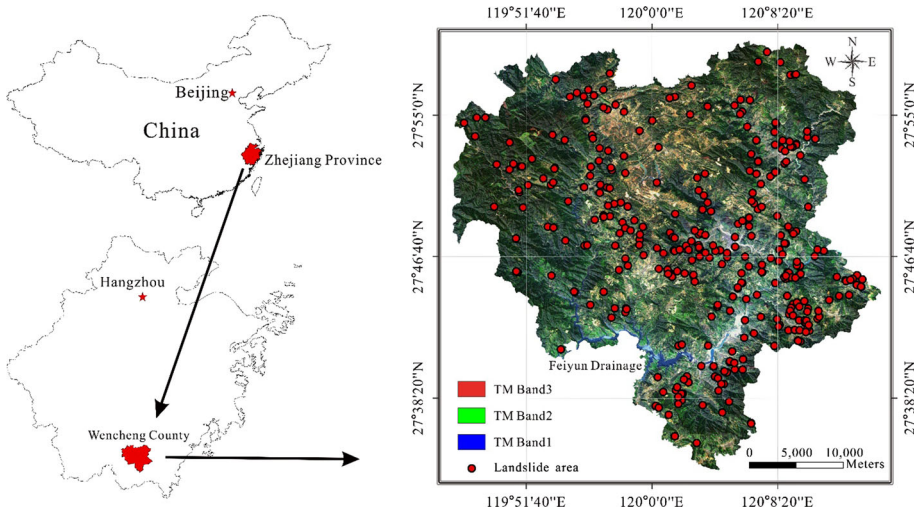


Fig. 1 Study area

300 and 111 mm, and cumulative precipitation of 332 and 150 mm, respectively, to Wencheng.

2 Study area

The Wencheng County study area is located in the southern part of Zhejiang Province in China. It covers approximately 1,296 km², lies between 27°34′–27°59′N and 119°46′–120°15′E (Fig. 1), and ranges in altitude from 10 to 1,350 m. The principal terrain of hills and mountains, of which 178 are over 1,000 m high, occupies about 95.4 % of the entire area, which can be divided into northern and southern parts by the Feiyun Drainage. The northern part belongs to the Luoshan Mountains, and the southern part is a branch of the southern Yandang Mountains. Only about 4.5 % of the study area has flat terrain, which lies along the Feiyun drainage networks (Zhu 1996). NW and NE faults and intrusions are well developed, and Mesozoic volcanic rocks of the Jurassic and Cretaceous periods are distributed widely within the study area. Exposed strata are mainly Quaternary, lower Cretaceous, and upper Jurassic. In the mountain areas, the stratum is mainly volcanoclastic rock, which is easily weathered to become the source of landslides. In the flat areas, the stratum, comprising mainly silty fine sand and clayey soil, has relatively good geological engineering condition (Geological Exploration bureau of Zhejiang Province 1989). Wencheng features a subtropical monsoon climate, and the weather is relatively moderate with an annual average temperature of 28–35 °C. Most of Wencheng’s rain is brought by the monsoon, falling in just a few weeks between April and September (Zhu 1999). The topography and climate make rainfall-induced landslides a common occurrence, which is why Wencheng was selected as a representative study area.

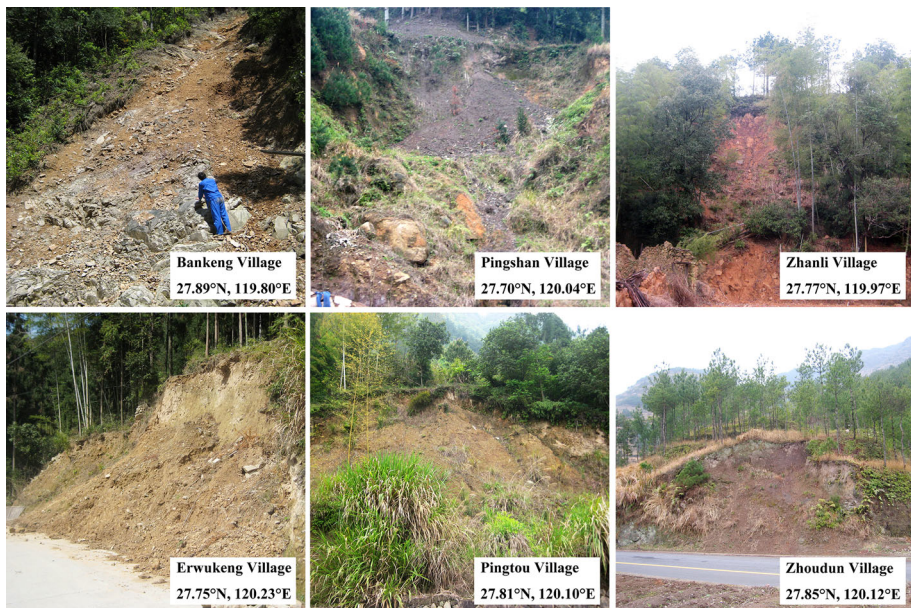


Fig. 2 Field photographs illustrating the characteristics and types of landslides in various parts of the study area

Table 1 Correlations between conditioning factors and landslide inventories

Conditioning factors	Lithology	Elevation	Distance to roads	NDVI	Land use	Slope	Aspect	Profile curvature	Distance to faults	Distance to drainage
η_{FL}	0.338	-0.284	-0.272	-0.188	-0.139	-0.098	0.050	0.031	-0.022	-0.005

3 Data

3.1 Landslide inventory

A landslide inventory map displays the location, time, characteristics, and other detailed information regarding the occurrence of a landslide, which is the most essential information for landslide susceptibility mapping, because any method requires such basic a priori knowledge. A survey by the Zhejiang Land Resources Bureau of China found 354 distinct landslide events had occurred within the study area from 1981 to 2010 (red dots in Fig. 1). According to landslide inventory records, all of these landslides were triggered by rainfall and their depths were shallow, which are the characteristics of interest in this study, as shown in Fig. 2. The training and test datasets were constructed by overlaying these 354

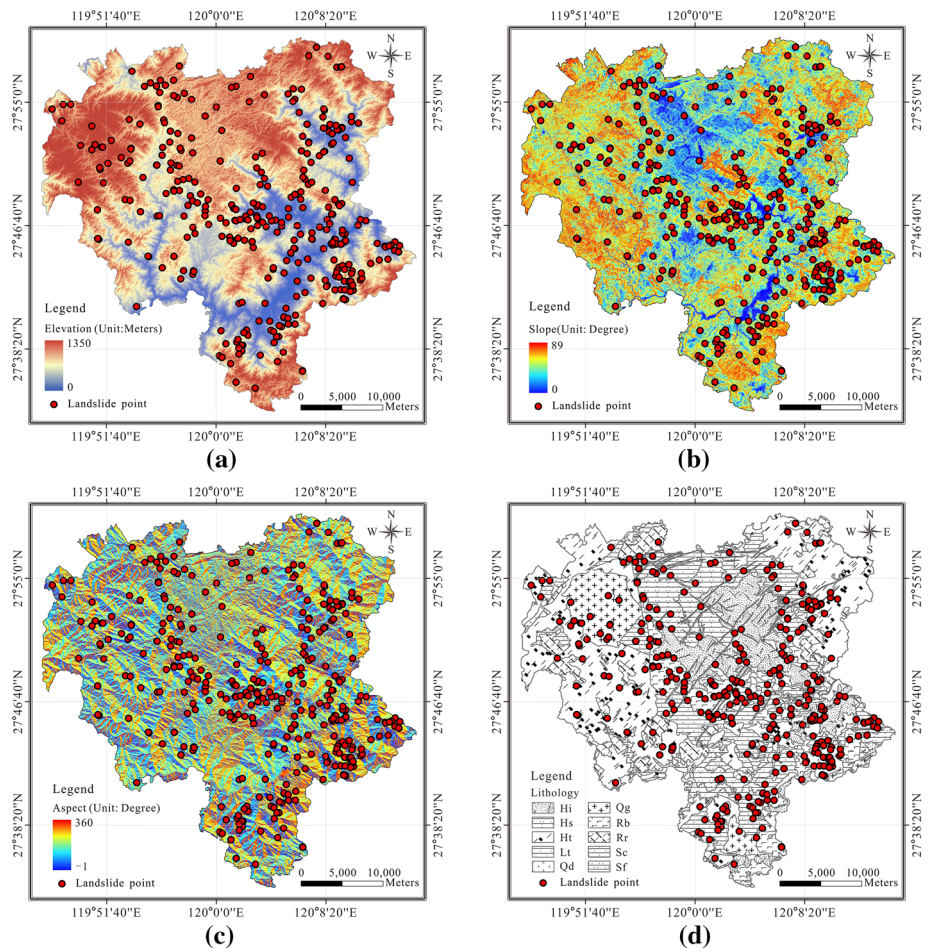


Fig. 3 Conditioning factors: **a** elevation, **b** slope, **c** aspect, **d** lithology, **e** NDVI, **f** land use, **g** distance to roads, and **h** distribution of meteorological stations

landslides with the selected conditioning and triggering factors, detailed in Sects. 3.2 and 3.3.

3.2 Landslide conditioning factors

Previous studies have examined the correlations between landslide occurrence and environmental parameters, such as slope, aspect, lithology, land use, vegetation, and groundwater (e.g., Dai and Lee 2002; Gómez and Kavzoglu 2005; Jebur et al. 2014). A landslide is caused by many factors and their extremely complex combination, but to some extent, the correlation coefficient could guide the selection of the most important factors. Based on the availability of data and the results of the correlation analyses between the data and landslide inventories using Eq. 1, as shown in Table 1, seven of the ten conditioning factors (lithology, elevation, distance to roads, normalized difference vegetation index (NDVI), land use, slope, and aspect) used in this study with relatively high correlation

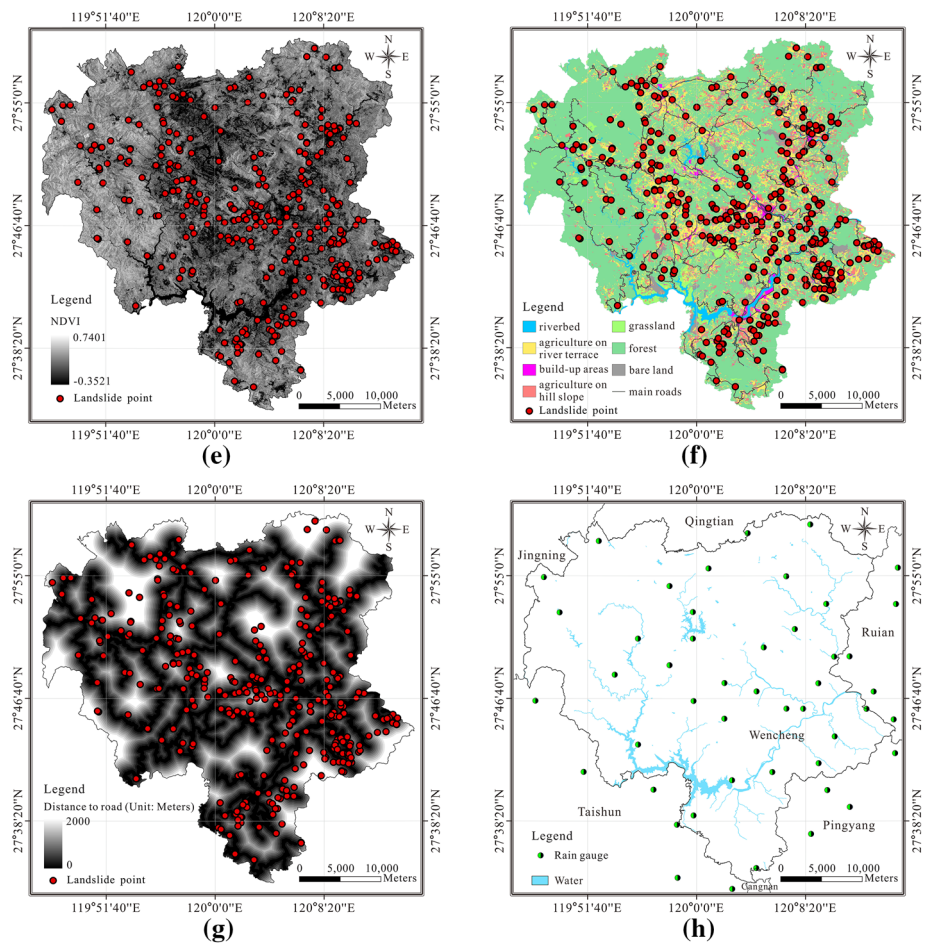


Fig. 3 continued

coefficients, fall into four categories (topographic, lithology, vegetation, and anthropogenic), as shown in Fig. 3.

$$\eta_{FL} = \frac{\text{cov}(F, L)}{\sigma_F \sigma_L} \quad (1)$$

where η_{FL} is the correlation coefficient of factor F and landslides L , $\text{cov}(F, L)$ is the covariance of F and L , and σ_F and σ_L are the standard deviations of F and L , respectively.

3.2.1 Topographic factors including elevation, slope, and aspect

All topographic factors were derived from the 1:10,000 contour map produced by the National Administration of Surveying, Mapping, and Geoinformation, China. Elevation not only influences a large number of biophysical parameters and anthropogenic activities, but it also has a significant effect on soil characteristics (e.g., texture and depth). Elevations within the study area range from 10 to 1,350 m, and 81 % of landslides occurred between elevations of 100 and 700 m, as shown in Fig. 3a.

Slope affects the velocity of both surface and subsurface flows, and consequently, it has influence on soil water content, soil formation, erosion potential, and a large number of important geomorphic processes. It has been noted that locations at which the slope is nearer to 0° are considered safer in terms of landslide initiation (Lee and Min 2001; Yilmaz 2009). The occurrence of landslides tends to increase with an increase of slope, but when the slope becomes near vertical, landslides are rare or absent because of the lack of soil development and deposit accumulation. In this study, nearly 86 % of the study area has slopes ranging from 6° to 46°. The mean slope is 27° and the maximum is 89°. About 79 % of the landslides occurred on slopes ranging from 10° to 35°, as shown in Fig. 3b.

Aspect encompasses the structural and basic organic conditions of a slope including fault planes and climatic factors (Dimri et al. 2007; Yalcin 2008). Larger numbers of landslides occur on wetter slopes with south-facing aspects than on drier slopes with north-facing aspects. An aspect value of −1° is frequently assigned to flat areas such as lakes and river. About 54 % of the landslides within the study area occurred on slopes with SE–SW aspects, as shown in Fig. 3c.

3.2.2 Lithology

Lithology is one of the most important factors in landslides. Different lithologies have different physical and chemical properties, which result in differing strengths and permeabilities of the underlying rocks. Lithological data were compiled from a 1:10,000 geological map produced by Ministry of Land and Resources of China. These were aggregated into ten categories, as shown in Fig. 3d: acidic rhyolite (Rr), fine-grained clastic rocks dominated by siltstone and mudstone (Sf), vitric and crystal tuff (Ht), ignimbrite (Hi), acidic granite (Qg), tuffaceous claystone (Hs), coarse clastic rocks dominated by sandstone and conglomerate (Sc), gravel soil (Lt), mafic basalt (Rb), and neutral diorite (Qd). In the study, landslides occurred principally in Sc (25 %), Rb (23 %), and Ht (17 %) lithologies (Geological Exploration Bureau of Zhejiang Province 1989).

3.2.3 Vegetation

Vegetation cover plays an important role in the occurrence of landslides through the influence of root cohesion and moisture retention (Lee and Min 2001; Pourghasemi et al. 2014). The NDVI, derived from a TM remote sensing image using Eq. 2, was selected to represent the vegetation in this study, as shown in Fig. 3e. Landslides in the study area often occurred in summer during days with heavy rainfall; therefore, a TM image from June 15, 2009 was selected. In addition, because changes of vegetation are not obvious within the mass, vegetation is considered a type of constant variable. Only one TM remote sensing image was used to produce the NDVI, which ranged from -0.4 to 0.7 ; about 84 % of landslides occurred in areas with values of NDVI from 0.3 to 0.6.

$$\text{NDVI} = \frac{(\text{IR} - \text{R})}{(\text{IR} + \text{R})} \quad (2)$$

where IR represents band 4 and R represents band 3 of the TM images.

3.2.4 Anthropogenic factors including land use and distance to roads

It is known that land use is one of the parameters most sensitive to environmental change, especially artificial effects such as road cuts and construction activities (Dahal 2014; Yalcin 2008), because landslides often occurred besides houses and roads in the study area. Based on a 1:10,000 land use map produced by the Ministry of Land and Resources of China, the various land uses were grouped into seven principal classes, as shown in Fig. 3f: forest, grassland, agriculture on river terraces, agriculture on hill slopes, built-up areas, bare land, and riverbeds. In the study, landslides occurred principally in areas of forest (45 %), agriculture on river terraces (19 %), agriculture on hill slopes (17 %), and built-up areas (17 %).

Road construction in hilly areas can alter slope stability considerably, making them vulnerable to slope instability and landslides. Therefore, in this study, main roads with widths greater than 15 m were interpreted from 1-m-resolution aerial photographs produced by the National Administration of Surveying, Mapping, and Geoinformation, China, in 2003. The distance to the roads of each pixel with spatial resolution of 30 m was calculated, which indicated that 87 % of landslides occurred within 100 m of a road, as shown in Fig. 3f.

3.3 Landslide triggering factors

Rainfall is the most common triggering factor for landslides. In this study, the two parameters of daily and cumulative precipitation are considered in describing the rainfall event. To obtain precise rainfall data, daily precipitation data were collected for the 30-year period from January 1, 1981, to December 31, 2010. These data were obtained from 47 meteorological stations, operated by the Meteorological Bureau of Zhejiang, China, and distributed around the study area, as shown in Fig. 3h.

To compile the rainfall data as triggering factors for the mapping of landslide susceptibility, 10,957 [365 (days) multiplied by 30 (years) plus 7 (additional days because of leap years between 1981 and 2010)] maps of daily precipitation of the study area with 30-m spatial resolution were produced by Kriging interpolation.

Table 2 Correlations between cumulative precipitation and landslide inventories with different values of k and n in Eq. 3

k	n	2	3	4	5	6	7	8	9	10	11	12	13	14	15
0.1	0.6744	0.6744	0.6744	0.6744	0.6744	0.6744	0.6744	0.6744	0.6744	0.6744	0.6744	0.6744	0.6744	0.6744	0.6744
0.2	0.6788	0.6788	0.6789	0.6789	0.6789	0.6789	0.6789	0.6789	0.6789	0.6789	0.6789	0.6789	0.6789	0.6789	0.6789
0.3	0.6823	0.6824	0.6825	0.6825	0.6825	0.6825	0.6825	0.6825	0.6825	0.6825	0.6825	0.6825	0.6825	0.6825	0.6825
0.4	0.6848	0.6851	0.6854	0.6853	0.6853	0.6853	0.6853	0.6853	0.6853	0.6853	0.6853	0.6853	0.6853	0.6853	0.6853
0.5	0.6863	0.6867	0.6874	0.6872	0.6871	0.6871	0.6871	0.6870	0.6870	0.6870	0.6870	0.6870	0.6870	0.6870	0.6870
0.6	0.6869	0.6872	0.6884	0.6879	0.6876	0.6876	0.6874	0.6871	0.6869	0.6869	0.6869	0.6869	0.6869	0.6870	0.6870
0.7	0.6865	0.6864	0.6881	0.6868	0.6857	0.6857	0.6852	0.6840	0.6834	0.6835	0.6834	0.6834	0.6836	0.6838	0.6839
0.8	0.6851	0.6841	0.6857	0.6826	0.6799	0.6799	0.6782	0.6743	0.6720	0.6721	0.6719	0.6720	0.6728	0.6743	0.6747
0.9	0.6827	0.6799	0.6799	0.6733	0.6666	0.6666	0.6618	0.6503	0.6420	0.6410	0.6394	0.6397	0.6434	0.6507	0.6329
1.0	0.6793	0.6735	0.6691	0.6559	0.6409	0.6409	0.6278	0.5956	0.5688	0.5588	0.5504	0.5493	0.5631	0.5875	0.5971

Based on these daily precipitation maps, the cumulative precipitation maps were derived using Eq. 3 (Glade et al. 2000).

$$P_a = r_0 + kr_1 + k^2r_2 + \dots + k^n r_n \tag{3}$$

where P_a is cumulative precipitation, r_i is daily precipitation on the i -th day preceding the landslide event ($1 \leq i \leq n$), and k is a decay coefficient related to evaporation.

To determine parameters k and n in Eq. 3, the cumulative precipitation was calculated for a day between 1981 and 2010 on which a landslide occurred, selected randomly, and the different values of k and n established to analyze the correlations of the landslide inventories. This process was repeated ten times to provide the average correlations presented in Table 2. Based on the results, the values of k and n in Eq. 3 were identified as 0.6 and 4, because they provide the maximum correlation of landslides in this study.

3.4 Negative samples (areas not prone to slides)

The mapping of landslide susceptibility aims to identify those areas prone to slide and those areas not, which can be considered as a classification issue requiring a priori knowledge of positive samples (landslide inventories defined as class 1) and negative samples (areas not prone to slide defined as class -1). It is obvious that class imbalance and sampling bias will significantly influence the results of the classification. Therefore, the number of negative samples has to be similar to the number and distribution of positive samples. To select appropriate negative samples, the seven factors (conditioning factors related to landslide inventories) were overlaid and the study area divided into 11,332,286 units with 1,048,576 factor combination patterns. Those units with combination patterns of

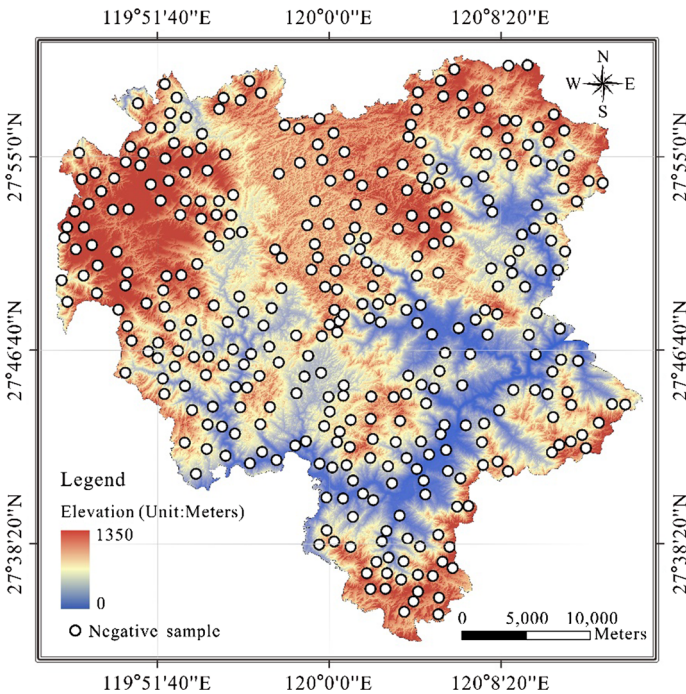


Fig. 4 Distribution of negative samples (areas not prone to slide)

landslide inventories were removed first to avoid conflict in the selection of the negative samples. Then, the remaining units were sorted according to area and small units; about 25 % of the areas were removed from smallest to largest because they were considered small probability events. After removing the small units, 354 negative samples, which were considered as representative areas not prone to slide, were selected randomly, i.e., the same number as the landslide inventories, as shown in Fig. 4.

4 Methodology

4.1 Support vector machine (SVM)

SVM is a machine learning technique for two class (+1 and -1; areas prone to slides and areas not prone to slides in this study) classification based on the concept of an optimal separating hyperplane developed by Cortes and Vapnik (1995). The basic theory behind SVM is to seek the maximum margin of separation between the two classes in the original n -dimensional space and to find the separating hyperplane in the middle of the maximum margin, which minimizes the structural risk, from the training dataset including both positive and negative sample points. Each point x in the n -dimensional space is classified as +1 where it lies above the hyperplane; otherwise, it is classified as -1. The specific classification function is given by Eq. 4, where y is the class label, sgn is a sign function, and \mathbf{W} and b are the parameters of the hyperplane. To resolve the hyperplane, the issue of seeking the maximum margin can be described by Eq. 5. However, in practice, no hyperplane could guarantee that all the sample points in the training dataset could be separated correctly. Therefore, a slack variable $\zeta_i \geq 0$ is invoked in Eq. 5 to satisfy the condition (see Eq. 6), where C is a penalty coefficient that is bigger for those sample points incorrectly separated.

To resolve landslide susceptibility mapping, which is a nonlinear issue, the kernel trick (Scholkopf 2001) is applied in SVM, which is that the dot product $\phi(x) \cdot \phi(y)$ can represent the kernel function $K(x, y)$ when the projection $\phi: X \rightarrow H$ from the original space X to a space H . Therefore, Eq. 4 can be written as Eq. 7. In this study, the radial basis function Gaussian kernel function, suggested by Hsu et al. (2003), is used, because it has good generalizing properties (see Eq. 8).

$$y = \text{sgn}(\mathbf{W} \cdot \mathbf{x} + b). \tag{4}$$

$$\left. \begin{aligned} \min \quad & \frac{1}{2} \|\mathbf{w}\|^2, \\ \text{s.t.} \quad & y_i[(\mathbf{w} \cdot x_i) + b] \geq 1. \end{aligned} \right\} \tag{5}$$

$$\left. \begin{aligned} \min \quad & \frac{1}{2} \|\mathbf{w}\|^2 + C \sum_{i=1}^N \zeta_i, \\ \text{s.t.} \quad & \begin{cases} y_i[(\mathbf{w} \cdot x_i) + b] \geq 1 - \zeta_i; \\ \zeta_i \geq 0; \\ C > 0. \end{cases} \end{aligned} \right\} \tag{6}$$

$$y = \text{sgn} \left(\sum_1^N \alpha_i K(x_i, x_j) + b \right). \tag{7}$$

$$K(x, y) = \exp\left(-\gamma\|x - y\|^2\right). \tag{8}$$

4.2 Implementation of SVM models

In this study, LIBSVM 3.18 (Chang and Lin 2011) was employed for the SVM analyses. The conditioning and triggering factors were derived as regular grid raster data with spatial resolution of 30 m using GIS. As shown in Table 3, the categorical variables including aspect, land use, and lithology were enumerated, and the continuous variables of elevation, slope, NDVI, distance to roads, direct daily precipitation, and cumulative precipitation were graded according to certain intervals. To eliminate the influence of the different class number of the factors, each factor was normalized to [0, 1].

To find the optimal parameter, an iterative grid search is applied in which the evaluation is provided by a fivefold cross-validation, detailed in Sect. 4.3. The range of γ and C in Eqs. 8 and 7 was set to $[-1,024, 1,024]$, and the step was 0.01. Based on the search, the values of the parameters were determined as $\gamma = 1.23$ and $C = 1.27$, as shown in Fig. 5.

Because SVM is a classifier for two classes, its result usually is an integer label such as +1 or -1 (i.e., in this study, prone to slide or not prone to slide). To acquire smooth floating values of landslide susceptibilities, the sigmoid transformation using Eq. 9 (Platt 1999) is applied to transform the distance to the hyperplane in the SVM model into the landslide susceptibility for each pixel in this study area. According to the transformation result and based on our experience of the landslide inventories, the landslide susceptibility in Wencheng can be divided into four levels: no susceptibility (<0.5), low susceptibility (0.5–0.75), moderate susceptibility (0.75–0.9), and high susceptibility (>0.9).

Table 3 Datasets and their classes for this study

Dataset	Classes
Elevation (m)	(1) <90; (2) 90–180; (3) 180–270; (4) 270–360; (5) 360–450; (6) 450–540; (7) 540–630; (8) 630–720; (9) 720–810; (10) 810–900; (11) 900–990; (12) 990–1,080; (13) 1,080–1,170; (14) 1,170–1,260; (15) >1,260
Slope (°)	(1) <5; (2) 5–10; (3) 10–15; (4) 15–20; (5) 20–25; (6) 25–30; (7) 30–35; (8) 35–40; (9) 40–45; (10) 45–50; (11) 50–55; (12) 55–60; (13) 60–65; (14) 65–70; (15) 70–75; (16) 75–80; (17) 80–85; (18) 85–90
Aspect	(1) Flat; (2) N; (3) NE; (4) E; (5) SE; (6) S; (7) SW; (8) W; (9) NW
NDVI	(1) <-0.3; (2) -0.3 to -0.2; (3) -0.2 to -0.1; (4) -0.1 to -0.0; (5) 0.0 to 0.1; (6) 0.1 to 0.2; (7) 0.2 to 0.3; (8) 0.3 to 0.4; (9) 0.4 to 0.5; (10) 0.5 to 0.6; (11) 0.6 to 0.7; (12) >0.7
Lithology	(1) Rr; (2) Sf; (3) Ht; (4) Hi; (5) Qg; (6) Hs; (7) Sc; (8) Lt; (9) Rb; (10) Qd
Land use	(1) Riverbed; (2) agriculture on river terraces; (3) built-up areas; (4) agriculture on hill slopes; (5) grassland; (6) forest; (7) bare land
Daily precipitation (mm)	(1) <20; (2) 20–40; (3) 40–60; (4) 60–80; (5) 80–100; (6) 100–120; (7) 120–140; (8) 140–160; (9) 160–180; (10) 180–200; (11) 200–220; (12) 220–240; (13) 240–260; (14) 260–280; (15) 280–300; (16) 300–320; (17) >320
Cumulative precipitation (mm)	(1) <30; (2) 30–60; (3) 60–90; (4) 90–120; (5) 120–150; (6) 150–180; (7) 180–210; (8) 210–240; (9) 240–270; (10) 270–300; (11) 300–330; (12) 330–360; (13) 360–390; (14) 390–420; (15) >420

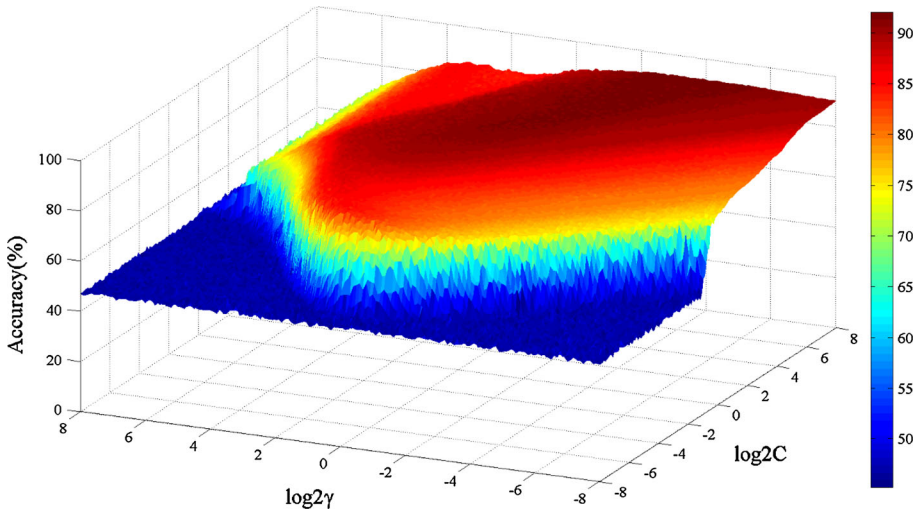


Fig. 5 Grid search for parameters γ and C

$$p(y = 1|x) = \frac{1}{(1 + \exp(a \cdot f(x) + b))} \tag{9}$$

where a and b are constants, whose values of -0.8308 and 0.3279 , respectively, were chosen to maximize the negative log-likelihood.

4.3 Model performance evaluation

In landslide susceptibility mapping work, landslide inventories as a priori knowledge are usually rare because landslides are unusual events in daily life. To eliminate the impact of the construction of the training dataset, in this paper, the original dataset (708 points comprising 354 positive and 354 negative sample points) was not divided into a training dataset and a validation dataset, but instead, a fivefold cross-validation was applied (Kohavi 1995). In the fivefold cross-validation, the original dataset was divided into five random subdatasets of equal size. One of the subdatasets was retained as the validation dataset, and the remaining four used as the training dataset. Then, the cross-validation process was repeated five times with each subdataset used once as the validation dataset and the five validation results averaged to produce the final result.

To evaluate the performance of the SVM model in this study, the ROC (Fielding and Bell 1997) graph and prediction rate curve were applied, which provide useful information on the binary classifier system because its discrimination threshold is varied. The ROC graph is built by plotting the ratio between the true and false positives, resulting in a set of ROC curves. The performance is summarized by the area under the curve (AUC) (Fawcett 2006) related to the plot area, which indicates a complete success in the classification for the AUC with a value of 1, and a random classification with a value of 0.5.

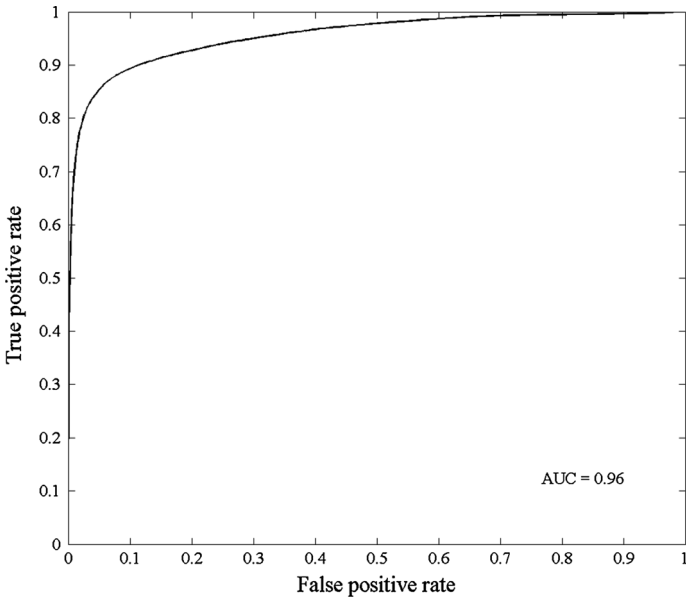


Fig. 6 Success rate curves for the susceptibility maps produced by SVM using fivefold cross-validation

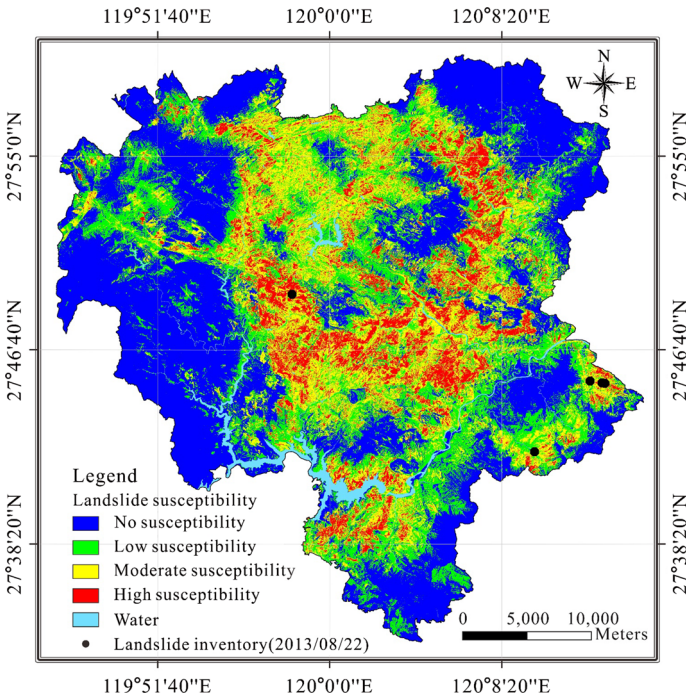


Fig. 7 Landslide susceptibility map on August 22, 2013

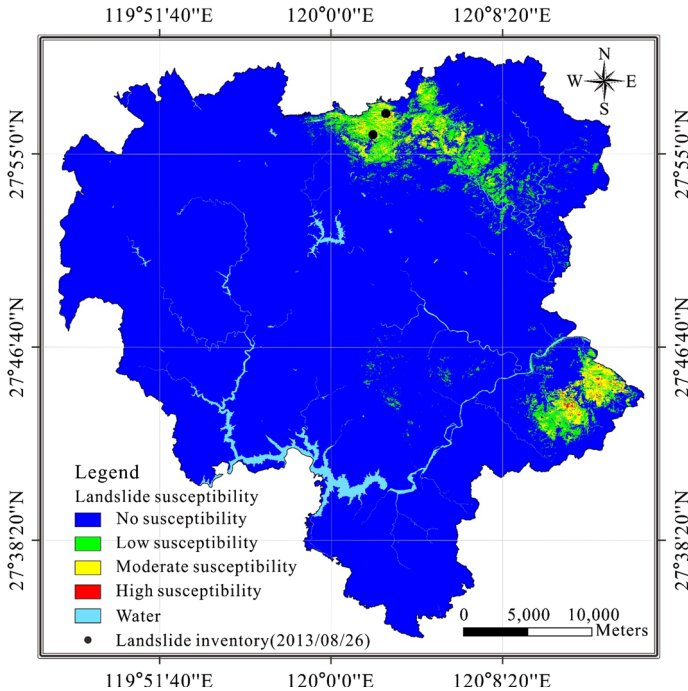


Fig. 8 Landslide susceptibility map on August 26, 2013

5 Results

To test the reliability of the SVM model, fivefold cross-validation and ROC analyses were used. First, 708 samples including 354 positive samples and 354 negative were divided randomly into five groups. Four groups of samples were used for training, and the remaining group used for validation. This procedure was repeated five times to obtain five results that were averaged to produce the final result. As illustrated by the ROC curve shown in Fig. 6, the SVM model has good performance for landslide susceptibility mapping, because the AUC is 0.96.

Two practical cases were investigated to evaluate the efficacy of the landslide susceptibility mapping, as shown in Fig. 7 for Trami typhoon on August 22, 2013, and in Fig. 8 for the Kong-Re typhoon of August 26, 2013. The landslide susceptibility for each point in this study area is calculated by the distance to the classification hyperplane in the SVM model (Platt 1999) and divided into four grades using an identical standard according to empirical analyses. Specifically, when the landslide susceptibility is less than 0.5, the point is defined as having no susceptibility; values of 0.5–0.75 represent low susceptibility, 0.75–0.9 indicate moderate susceptibility, and values over 0.9 represent high susceptibility. The results demonstrate that the SVM model produces high probability values over a small area. For example, on August 22, the landslide susceptibility map confines the fourth grade (area prone to slides with highest probability) to within 20 % of the study area, and on August 26, the map confines the fourth grade to within 15 %. In addition, note that all landslides occurred in those areas labeled as fourth or third grade in the result map.

Furthermore, if the triggering factor (i.e., rainfall data) was replaced by weather forecast data, the landslide susceptibility mapping could be converted into landslide warning.

6 Conclusions

A landslide susceptibility map is one of the most important pieces of information for planning agencies when a planning policy is to be implemented and for governments intending to reduce the socioeconomic costs of such hazards. In this study, the SVM model has been applied successfully for the mapping of rainfall-induced landslide susceptibility in the Wencheng area of Zhejiang Province in China. The model used seven conditioning factors comprising elevation, slope, aspect, distance to roads, lithology, land use, and NDVI, and two triggering factors: daily and cumulative rainfall data. The training dataset for the SVM was constructed from 354 landslide inventories defined by field survey, and 354 points defining areas not prone to slides, selected based on the statistics of overlaid factors. An iterative grid search was applied to find the optimal parameters for the model. For result verification, a fivefold cross-validation and ROC analysis were used. The validation results showed that the SVM model could provide good and stable outcomes for which the AUC was 0.96. In addition, two practical cases focusing on typhoons Trami and Kong-Re were investigated. This revealed that SVM exhibited properties of stability and generalization and could provide a map in which high probability values were confined to a small area. Furthermore, landslide susceptibility mapping could be converted easily into landslide warning using weather forecasting data to replace the triggering factor; hence, policy makers, planners could make and publish the landslide warning and emergency plan to reduce losses of disasters. And engineers, geologists could give their professional advice for construction works and disaster management using the model based on the rainfall history. Therefore, SVM is proven a useful tool for landslide susceptibility mapping, and the results obtained from this study could be of benefit to policy planning in this area, reducing the damage caused by landslides.

Acknowledgments The authors would like to thank the three anonymous reviewers for their helpful reviews on the manuscript. Thanks are also expressed to the Zhejiang Land Resources Bureau of China for supporting this study.

References

- Akgun A, Dag S, Bulut F (2008) Landslide susceptibility mapping for a landslide-prone area (Findikli, NE of Turkey) by likelihood-frequency ratio and weighted linear combination models. *Environ Geol* 54:1127–1143. doi:[10.1007/s00254-007-0882-8](https://doi.org/10.1007/s00254-007-0882-8)
- Akgun A, Sezer EA, Nefeslioglu HA, Gokceoglu C, Pradhan B (2012) An easy-to-use MATLAB program (MamLand) for the assessment of landslide susceptibility using a Mamdani fuzzy algorithm. *Comput Geosci* 38:23–34. doi:[10.1016/j.cageo.2011.04.012](https://doi.org/10.1016/j.cageo.2011.04.012)
- Aleotti P, Chowdhury R (1999) Landslide hazard assessment: summary review and new perspectives. *Bull Eng Geol Environ* 58:21–44
- Althuwaynee OF, Pradhan B, Lee S (2012) Application of an evidential belief function model in landslide susceptibility mapping. *Comput Geosci* 44:120–135. doi:[10.1016/j.cageo.2012.03.003](https://doi.org/10.1016/j.cageo.2012.03.003)
- Althuwaynee OF, Pradhan B, Park H-J, Lee JH (2014a) A novel ensemble bivariate statistical evidential belief function with knowledge-based analytical hierarchy process and multivariate logistic regression for landslide susceptibility mapping. *Catena* 114:21–36. doi:[10.1016/j.catena.2013.10.011](https://doi.org/10.1016/j.catena.2013.10.011)

- Althuwaynee OF, Pradhan B, Park H-J, Lee JH (2014b) A novel ensemble decision tree-based Chi-squared Automatic Interaction Detection (CHAID) and multivariate logistic regression models in landslide susceptibility mapping. *Landslides* 11:1063–1078. doi:[10.1007/s10346-014-0466-0](https://doi.org/10.1007/s10346-014-0466-0)
- Ayalew L, Yamagishi H (2005) The application of GIS-based logistic regression for landslide susceptibility mapping in the Kakuda–Yahiko Mountains, Central Japan. *Geomorphology* 65:15–31. doi:[10.1016/j.geomorph.2004.06.010](https://doi.org/10.1016/j.geomorph.2004.06.010)
- Baeza C, Corominas J (2001) Assessment of shallow landslide susceptibility by means of multivariate statistical techniques. *Earth Surf Proc Land* 26:1251–1263. doi:[10.1002/esp.263](https://doi.org/10.1002/esp.263)
- Bai S-B, Wang J, Lü G-N, Zhou P-G, Hou S-S, Xu S-N (2010) GIS-based logistic regression for landslide susceptibility mapping of the Zhongxian segment in the three Gorges area, China. *Geomorphology* 115:23–31. doi:[10.1016/j.geomorph.2009.09.025](https://doi.org/10.1016/j.geomorph.2009.09.025)
- Ballabio C, Sterlacchini S (2012) Support vector machines for landslide susceptibility mapping: the Staffora River Basin case study, Italy. *Math Geosci* 44:47–70. doi:[10.1007/s11004-011-9379-9](https://doi.org/10.1007/s11004-011-9379-9)
- Brenning A (2005) Spatial prediction models for landslide hazards: review, comparison and evaluation. *Nat Hazards Earth Sys* 5:853–862
- Carrara A, Cardinali M, Detti R, Guzzetti F, Pasqui V, Reichenbach P (1991) GIS techniques and statistical models in evaluating landslide hazard. *Earth Surf Proc Land* 16:427–445
- Carrara A, Cardinali M, Guzzetti F, Reichenbach P (1995) GIS technology in mapping landslide hazard. In: Carrara A, Guzzetti F (eds) *Geographical information systems in assessing natural hazards*, vol 5. Springer, Netherlands, pp 135–175. doi:[10.1007/978-94-015-8404-3_8](https://doi.org/10.1007/978-94-015-8404-3_8)
- Carrara A, Crosta G, Frattini P (2003) Geomorphological and historical data in assessing landslide hazard. *Earth Surf Proc Land* 28:1125–1142. doi:[10.1002/esp.545](https://doi.org/10.1002/esp.545)
- Chacón J, Irigaray C, Fernández T, El Hamdouni R (2006) Engineering geology maps: landslides and geographical information systems. *Bull Eng Geol Environ* 65:341–411. doi:[10.1007/s10064-006-0064-z](https://doi.org/10.1007/s10064-006-0064-z)
- Chang K-T, Chiang S-H (2009) An integrated model for predicting rainfall-induced landslides. *Geomorphology* 105:366–373
- Chang C-C, Lin C-J (2011) LIBSVM: a library for support vector machines. *ACM Trans Intell Syst Technol (TIST)* 2:27
- Chang K, Chiang SH, Lei F (2008) Analysing the relationship between typhoon-triggered landslides and critical rainfall conditions. *Earth Surf Proc Land* 33:1261–1271
- Chau KT, Sze YL, Fung MK, Wong WY, Fong EL, Chan LCP (2004) Landslide hazard analysis for Hong Kong using landslide inventory and GIS. *Comput Geosci* 30:429–443. doi:[10.1016/j.cageo.2003.08.013](https://doi.org/10.1016/j.cageo.2003.08.013)
- Choi J, Oh H-J, Lee H-J, Lee C, Lee S (2012) Combining landslide susceptibility maps obtained from frequency ratio, logistic regression, and artificial neural network models using ASTER images and GIS. *Eng Geol* 124:12–23. doi:[10.1016/j.enggeo.2011.09.011](https://doi.org/10.1016/j.enggeo.2011.09.011)
- Corominas J, Moya J (2008) A review of assessing landslide frequency for hazard zoning purposes. *Eng Geol* 102:193–213. doi:[10.1016/j.enggeo.2008.03.018](https://doi.org/10.1016/j.enggeo.2008.03.018)
- Cortes C, Vapnik V (1995) Support-vector networks. *Mach Learn* 20:273–297
- Dahal RK (2014) Regional-scale landslide activity and landslide susceptibility zonation in the Nepal Himalaya. *Environ Earth Sci* 71:5145–5164
- Dahal RK, Hasegawa S, Nonomura A, Yamanaka M, Masuda T, Nishino K (2008) GIS-based weights-of-evidence modelling of rainfall-induced landslides in small catchments for landslide susceptibility mapping. *Environ Geol* 54:311–324
- Dai FC, Lee CF (2002) Landslide characteristics and slope instability modeling using GIS, Lantau Island, Hong Kong. *Geomorphology* 42:213–228. doi:[10.1016/S0169-555X\(01\)00087-3](https://doi.org/10.1016/S0169-555X(01)00087-3)
- Das I, Sahoo S, van Westen C, Stein A, Hack R (2010) Landslide susceptibility assessment using logistic regression and its comparison with a rock mass classification system, along a road section in the northern Himalayas (India). *Geomorphology* 114:627–637
- Devkota K et al (2013) Landslide susceptibility mapping using certainty factor, index of entropy and logistic regression models in GIS and their comparison at Mugling–Narayanghat road section in Nepal Himalaya. *Nat Hazards* 65:135–165. doi:[10.1007/s11069-012-0347-6](https://doi.org/10.1007/s11069-012-0347-6)
- Dimri S, Lakhera R, Sati S (2007) Fuzzy-based method for landslide hazard assessment in active seismic zone of Himalaya. *Landslides* 4:101–111
- Ercanoglu M, Gokceoglu C (2002) Assessment of landslide susceptibility for a landslide-prone area (north of Yenice, NW Turkey) by fuzzy approach. *Environ Geol* 41:720–730. doi:[10.1007/s00254-001-0454-2](https://doi.org/10.1007/s00254-001-0454-2)
- Ermini L, Catani F, Casagli N (2005) Artificial neural networks applied to landslide susceptibility assessment. *Geomorphology* 66:327–343. doi:[10.1016/j.geomorph.2004.09.025](https://doi.org/10.1016/j.geomorph.2004.09.025)

- Falaschi F, Giacomelli F, Federici PR, Puccinelli A, D'Amato Avanzi G, Pochini A, Ribolini A (2009) Logistic regression versus artificial neural networks: landslide susceptibility evaluation in a sample area of the Serchio River valley, Italy. *Nat Hazards* 50:551–569. doi:[10.1007/s11069-009-9356-5](https://doi.org/10.1007/s11069-009-9356-5)
- Fawcett T (2006) An introduction to ROC analysis. *Pattern Recogn Lett* 27:861–874
- Fielding AH, Bell JF (1997) A review of methods for the assessment of prediction errors in conservation presence/absence models. *Environ Conserv* 24:38–49
- Geological Exploration Bureau of Zhejiang Province (1989) Regional geology of Zhejiang Province. Geology Publishing House, Beijing (in Chinese)
- Glade T, Crozier M, Smith P (2000) Applying probability determination to refine landslide-triggering rainfall thresholds using an empirical “Antecedent Daily Rainfall Model”. *Pure Appl Geophys* 157:1059–1079. doi:[10.1007/s000240050017](https://doi.org/10.1007/s000240050017)
- Gómez H, Kavzoglu T (2005) Assessment of shallow landslide susceptibility using artificial neural networks in Jabonosa River Basin, Venezuela. *Eng Geol* 78:11–27. doi:[10.1016/j.enggeo.2004.10.004](https://doi.org/10.1016/j.enggeo.2004.10.004)
- Guo Q, Kelly M, Graham CH (2005) Support vector machines for predicting distribution of Sudden Oak Death in California. *Ecol Model* 182:75–90. doi:[10.1016/j.ecolmodel.2004.07.012](https://doi.org/10.1016/j.ecolmodel.2004.07.012)
- Guzzetti F, Carrara A, Cardinali M, Reichenbach P (1999) Landslide hazard evaluation: a review of current techniques and their application in a multi-scale study, Central Italy. *Geomorphology* 31:181–216. doi:[10.1016/S0169-555X\(99\)00078-1](https://doi.org/10.1016/S0169-555X(99)00078-1)
- Hong Y, Adler R, Huffman G (2007) Use of satellite remote sensing data in the mapping of global landslide susceptibility. *Nat Hazards* 43:245–256. doi:[10.1007/s11069-006-9104-z](https://doi.org/10.1007/s11069-006-9104-z)
- Hsu C-W, Chang C-C, Lin C-J (2003) A practical guide to support vector classification. Technical report. Department of Computer Science, National Taiwan University. <http://www.csie.ntu.edu.tw/~cjlin/papers/guide/guide.pdf>
- Jebur MN, Pradhan B, Tehrany MS (2014) Optimization of landslide conditioning factors using very high-resolution airborne laser scanning (LiDAR) data at catchment scale. *Remote Sens Environ* 152:150–165. doi:[10.1016/j.rse.2014.05.013](https://doi.org/10.1016/j.rse.2014.05.013)
- Kanungo DP, Arora MK, Sarkar S, Gupta RP (2006) A comparative study of conventional, ANN black box, fuzzy and combined neural and fuzzy weighting procedures for landslide susceptibility zonation in Darjeeling Himalayas. *Eng Geol* 85:347–366. doi:[10.1016/j.enggeo.2006.03.004](https://doi.org/10.1016/j.enggeo.2006.03.004)
- Kayastha P, Dhital MR, Smedt F (2012) Landslide susceptibility mapping using the weight of evidence method in the Tinau watershed, Nepal. *Nat Hazards* 63:479–498. doi:[10.1007/s11069-012-0163-z](https://doi.org/10.1007/s11069-012-0163-z)
- Kohavi R (1995) A study of cross-validation and bootstrap for accuracy estimation and model selection. *IJCAI* 2:1137–1145
- Lee S (2005) Application of logistic regression model and its validation for landslide susceptibility mapping using GIS and remote sensing data. *Int J Remote Sens* 26:1477–1491. doi:[10.1080/01431160412331331012](https://doi.org/10.1080/01431160412331331012)
- Lee S, Min K (2001) Statistical analysis of landslide susceptibility at Yongin, Korea. *Environ Geol* 40:1095–1113
- Lee S, Pradhan B (2006) Probabilistic landslide hazards and risk mapping on Penang Island, Malaysia. *J Earth Syst Sci* 115:661–672. doi:[10.1007/s12040-006-0004-0](https://doi.org/10.1007/s12040-006-0004-0)
- Lee S, Pradhan B (2007) Landslide hazard mapping at Selangor, Malaysia using frequency ratio and logistic regression models. *Landslides* 4:33–41. doi:[10.1007/s10346-006-0047-y](https://doi.org/10.1007/s10346-006-0047-y)
- Lee S, Ryu J-H, Lee M-J, Won J-S (2006) The application of artificial neural networks to landslide susceptibility mapping at Janghung, Korea. *Math Geol* 38:199–220
- Marjanović M, Kovačević M, Bajat B, Voženilek V (2011) Landslide susceptibility assessment using SVM machine learning algorithm. *Eng Geol* 123:225–234. doi:[10.1016/j.enggeo.2011.09.006](https://doi.org/10.1016/j.enggeo.2011.09.006)
- Mohammady M, Pourghasemi HR, Pradhan B (2012) Landslide susceptibility mapping at Golestan Province, Iran: a comparison between frequency ratio, Dempster–Shafer, and weights-of-evidence models. *J Asian Earth Sci* 61:221–236. doi:[10.1016/j.jseaes.2012.10.005](https://doi.org/10.1016/j.jseaes.2012.10.005)
- Nandi A, Shakoor A (2010) A GIS-based landslide susceptibility evaluation using bivariate and multivariate statistical analyses. *Eng Geol* 110:11–20. doi:[10.1016/j.enggeo.2009.10.001](https://doi.org/10.1016/j.enggeo.2009.10.001)
- Nefeslioglu HA, Sezer E, Gokceoglu C, Bozkir AS, Duman TY (2010) Assessment of landslide susceptibility by decision trees in the metropolitan area of Istanbul, Turkey. *Math Probl Eng*. doi:[10.1155/2010/901095](https://doi.org/10.1155/2010/901095)
- Neuhäuser B, Terhorst B (2007) Landslide susceptibility assessment using “weights-of-evidence” applied to a study area at the Jurassic escarpment (SW-Germany). *Geomorphology* 86:12–24. doi:[10.1016/j.geomorph.2006.08.002](https://doi.org/10.1016/j.geomorph.2006.08.002)
- Nourani V, Pradhan B, Ghaffari H, Sharifi SS (2013) Landslide susceptibility mapping at Zonouz Plain, Iran using genetic programming and comparison with frequency ratio, logistic regression, and artificial neural network models. *Nat Hazards* 71:523–547. doi:[10.1007/s11069-013-0932-3](https://doi.org/10.1007/s11069-013-0932-3)

- Oh H-J, Lee S, Chotikasathien W, Kim C, Kwon J (2009) Predictive landslide susceptibility mapping using spatial information in the Pechabun area of Thailand. *Environ Geol* 57:641–651. doi:[10.1007/s00254-008-1342-9](https://doi.org/10.1007/s00254-008-1342-9)
- Ohlmacher GC, Davis JC (2003) Using multiple logistic regression and GIS technology to predict landslide hazard in Northeast Kansas, USA. *Eng Geol* 69:331–343. doi:[10.1016/s0013-7952\(03\)00069-3](https://doi.org/10.1016/s0013-7952(03)00069-3)
- Ozdemir A, Altural T (2013) A comparative study of frequency ratio, weights of evidence and logistic regression methods for landslide susceptibility mapping: Sultan Mountains, SW Turkey. *J Asian Earth Sci* 64:180–197. doi:[10.1016/j.jseaes.2012.12.014](https://doi.org/10.1016/j.jseaes.2012.12.014)
- Platt J (1999) Probabilistic outputs for support vector machines and comparisons to regularized likelihood methods. *Adv Large Margin Classif* 10:61–74
- Pourghasemi HR, Pradhan B, Gokceoglu C (2012) Application of fuzzy logic and analytical hierarchy process (AHP) to landslide susceptibility mapping at Haraz watershed, Iran. *Nat Hazards* 63:965–996. doi:[10.1007/s11069-012-0217-2](https://doi.org/10.1007/s11069-012-0217-2)
- Pourghasemi HR, Moradi HR, Aghda SMF (2013) Landslide susceptibility mapping by binary logistic regression, analytical hierarchy process, and statistical index models and assessment of their performances. *Nat Hazards* 69:749–779. doi:[10.1007/s11069-013-0728-5](https://doi.org/10.1007/s11069-013-0728-5)
- Pourghasemi H, Moradi H, Aghda SF, Gokceoglu C, Pradhan B (2014) GIS-based landslide susceptibility mapping with probabilistic likelihood ratio and spatial multi-criteria evaluation models (North of Tehran, Iran). *Arab J Geosci* 7:1857–1878
- Pradhan B (2011) Use of GIS-based fuzzy logic relations and its cross application to produce landslide susceptibility maps in three test areas in Malaysia. *Environ Earth Sci* 63:329–349. doi:[10.1007/s12665-010-0705-1](https://doi.org/10.1007/s12665-010-0705-1)
- Pradhan B (2013) A comparative study on the predictive ability of the decision tree, support vector machine and neuro-fuzzy models in landslide susceptibility mapping using GIS. *Comput Geosci* 51:350–365. doi:[10.1016/j.cageo.2012.08.023](https://doi.org/10.1016/j.cageo.2012.08.023)
- Pradhan B, Lee S (2010a) Delineation of landslide hazard areas on Penang Island, Malaysia, by using frequency ratio, logistic regression, and artificial neural network models. *Environ Earth Sci* 60:1037–1054. doi:[10.1007/s12665-009-0245-8](https://doi.org/10.1007/s12665-009-0245-8)
- Pradhan B, Lee S (2010b) Landslide susceptibility assessment and factor effect analysis: backpropagation artificial neural networks and their comparison with frequency ratio and bivariate logistic regression modelling. *Environ Model Softw* 25:747–759. doi:[10.1016/j.envsoft.2009.10.016](https://doi.org/10.1016/j.envsoft.2009.10.016)
- Pradhan B, Sezer EA, Gokceoglu C, Buchroithner MF (2010a) Landslide susceptibility mapping by neuro-fuzzy approach in a landslide-prone area (Cameron Highlands, Malaysia). *Geosci Remote Sens IEEE Trans* 48:4164–4177
- Pradhan B, Youssef A, Varathrajoo R (2010b) Approaches for delineating landslide hazard areas using different training sites in an advanced artificial neural network model. *Geo-Spat Inform Sci* 13:93–102. doi:[10.1007/s11806-010-0236-7](https://doi.org/10.1007/s11806-010-0236-7)
- Pradhan B, Mansor S, Pirasteh S, Buchroithner MF (2011) Landslide hazard and risk analyses at a landslide prone catchment area using statistical based geospatial model. *Int J Remote Sens* 32:4075–4087. doi:[10.1080/01431161.2010.484433](https://doi.org/10.1080/01431161.2010.484433)
- Saito H, Nakayama D, Matsuyama H (2009) Comparison of landslide susceptibility based on a decision-tree model and actual landslide occurrence: the Akaishi Mountains, Japan. *Geomorphology* 109:108–121. doi:[10.1016/j.geomorph.2009.02.026](https://doi.org/10.1016/j.geomorph.2009.02.026)
- Schicker R, Moon V (2012) Comparison of bivariate and multivariate statistical approaches in landslide susceptibility mapping at a regional scale. *Geomorphology* 161–162:40–57. doi:[10.1016/j.geomorph.2012.03.036](https://doi.org/10.1016/j.geomorph.2012.03.036)
- Scholkopf B (2001) The kernel trick for distances. *Adv Neural Inf Process Syst* 14:301–307
- Tangestani MH (2009) A comparative study of Dempster-Shafer and fuzzy models for landslide susceptibility mapping using a GIS: an experience from Zagros Mountains, SW Iran. *J Asian Earth Sci* 35:66–73. doi:[10.1016/j.jseaes.2009.01.002](https://doi.org/10.1016/j.jseaes.2009.01.002)
- Tehrany MS, Pradhan B, Jebur MN (2014) Flood susceptibility mapping using a novel ensemble weights-of-evidence and support vector machine models in GIS. *J Hydrol* 512:332–343. doi:[10.1016/j.jhydrol.2014.03.008](https://doi.org/10.1016/j.jhydrol.2014.03.008)
- Tien Bui D, Pradhan B, Lofman O, Revhaug I (2012a) Landslide susceptibility assessment in Vietnam using support vector machines, decision tree, and naive Bayes models. *Math Probl Eng* 2012:26. doi:[10.1155/2012/974638](https://doi.org/10.1155/2012/974638)
- Tien Bui D, Pradhan B, Lofman O, Revhaug I, Dick OB (2012b) Spatial prediction of landslide hazards in Hoa Binh Province (Vietnam): a comparative assessment of the efficacy of evidential belief functions and fuzzy logic models. *Catena* 96:28–40. doi:[10.1016/j.catena.2012.04.001](https://doi.org/10.1016/j.catena.2012.04.001)

- Umar Z, Pradhan B, Ahmad A, Jebur MN, Tehrany MS (2014) Earthquake-induced landslide susceptibility mapping using an integrated ensemble frequency ratio and logistic regression models in West Sumatera Province, Indonesia. *Catena* 118:124–135. doi:[10.1016/j.catena.2014.02.005](https://doi.org/10.1016/j.catena.2014.02.005)
- van den Eeckhaut M, Vanwalleggem T, Poesen J, Govers G, Verstraeten G, Vandekerckhove L (2006) Prediction of landslide susceptibility using rare events logistic regression: a case-study in the Flemish Ardennes (Belgium). *Geomorphology* 76:392–410. doi:[10.1016/j.geomorph.2005.12.003](https://doi.org/10.1016/j.geomorph.2005.12.003)
- van Westen CJ, Rengers N, Terlien M, Soeters R (1997) Prediction of the occurrence of slope instability phenomenal through GIS-based hazard zonation. *Geol Rundsch* 86:404–414
- van Westen CJ, Asch TWJ, Soeters R (2006) Landslide hazard and risk zonation—why is it still so difficult? *Bull Eng Geol Environ* 65:167–184. doi:[10.1007/s10064-005-0023-0](https://doi.org/10.1007/s10064-005-0023-0)
- van Westen CJ, Castellanos E, Kuriakose SL (2008) Spatial data for landslide susceptibility, hazard, and vulnerability assessment: an overview. *Eng Geol* 102:112–131. doi:[10.1016/j.enggeo.2008.03.010](https://doi.org/10.1016/j.enggeo.2008.03.010)
- Varnes DJ (1984) Landslide hazard zonation: a review of principles and practice, UNESCO, Paris. *Nat Hazards* 3:3–63
- Vijith H, Madhu G (2007) Estimating potential landslide sites of an upland sub-watershed in Western Ghat's of Kerala (India) through frequency ratio and GIS. *Environ Geol* 55:1397–1405. doi:[10.1007/s00254-007-1090-2](https://doi.org/10.1007/s00254-007-1090-2)
- Ward WH (1945) The stability of natural slopes. *Geogr J* 105:170–191
- Yalcin A (2008) GIS-based landslide susceptibility mapping using analytical hierarchy process and bivariate statistics in Ardesen (Turkey): comparisons of results and confirmations. *Catena* 72:1–12
- Yao X, Tham LG, Dai FC (2008) Landslide susceptibility mapping based on support vector machine: a case study on natural slopes of Hong Kong, China. *Geomorphology* 101:572–582. doi:[10.1016/j.geomorph.2008.02.011](https://doi.org/10.1016/j.geomorph.2008.02.011)
- Yeon Y-K, Han J-G, Ryu KH (2010) Landslide susceptibility mapping in Injae, Korea, using a decision tree. *Eng Geol* 116:274–283. doi:[10.1016/j.enggeo.2010.09.009](https://doi.org/10.1016/j.enggeo.2010.09.009)
- Yesilnacar E, Topal T (2005) Landslide susceptibility mapping: a comparison of logistic regression and neural networks methods in a medium scale study, Hendek region (Turkey). *Eng Geol* 79:251–266. doi:[10.1016/j.enggeo.2005.02.002](https://doi.org/10.1016/j.enggeo.2005.02.002)
- Yilmaz I (2009) Landslide susceptibility mapping using frequency ratio, logistic regression, artificial neural networks and their comparison: a case study from Kat landslides (Tokat—Turkey). *Comput Geosci* 35:1125–1138. doi:[10.1016/j.cageo.2008.08.007](https://doi.org/10.1016/j.cageo.2008.08.007)
- Yilmaz C, Topal T, Stizen ML (2012) GIS-based landslide susceptibility mapping using bivariate statistical analysis in Devrek (Zonguldak-Turkey). *Environ Earth Sci* 65:2161–2178
- Yuan L, Zhang Q, Li W, Zou L (2006) Debris flow hazard assessment based on support vector machine. In: *Geoscience and remote sensing symposium, 2006. IGARSS 2006. IEEE international conference on, July 31 2006–Aug. 4 2006*. pp 4221–4224. doi:[10.1109/IGARSS.2006.1083](https://doi.org/10.1109/IGARSS.2006.1083)
- Zêzere JL, de Brum Ferreira A, Rodrigues ML (1999) The role of conditioning and triggering factors in the occurrence of landslides: a case study in the area north of Lisbon (Portugal). *Geomorphology* 30:133–146. doi:[10.1016/S0169-555X\(99\)00050-1](https://doi.org/10.1016/S0169-555X(99)00050-1)
- Zhu L (1996) Wencheng county. Zhonghua Book Company, Beijing (in Chinese)
- Zhu MY (1999) Meteorology of Zhejiang province. Zhonghua Book Company, Beijing (in Chinese)